CHANGE IN THE WIND AND CLIMATE AT THE EXOMARS 2022 LANDING SITE IN OXIA PLANUM (MARS). S. Silvestro[1,2], D. Tirsch[3], A. Pacifici[4], F. Salese[5,4], D.A. Vaz[6], A. Neesemann[7], C.I. Popa[1], M. Pajola[8], G. Franzese[1], G. Mongelluzzo[1,9], A.C. Ruggeri[1], F. Cozzolino[1], C. Porto[1], F. Esposito[1]. [1]INAF, Osservatorio Astronomico di Capodimonte, Napoli, Italy (simone.silvestro@inaf.it). [2]SETI Institute, Carl Sagan Center, Mountain View, CA, USA. [3]Institute of Planetary Research, DLR, Berlin, Germany. [4]IRSPS, Università G. D'Annunzio, Pescara, Italy. [5]Centro de Astrobiología, CSIC-INTA, Madrid. [6]CESR University of Coimbra, Portugal. [7]Freie Universitat, Berlin, Germany. [8]INAF, Osservatorio Astronomico di Padova, Padova, Italy. [9]Department of Industrial Engineering, Università Federico II, Napoli, Italy.

Introduction: The ESA/ROSCOSMOS ExoMars 2022 (a rover named "Rosalind Franklin" and a surface platform named "Kazachok") [1] will land in Oxia Planum (18.2° N; 24.3° W) to search for signs of past or present life on Mars and to perform long-term atmospheric investigations [2,3]. Oxia Planum shows large outcrops of clay-rich Noachian-aged phyllosilicates [4,5]. The clay bearing unit is unconformably overlain by an Amazonian dark resistant unit (Adru), which was interpreted to be remnants of an Early Amazonian (2.6 Ga) volcanic material [4]. Aeolian megaripples (TARs/mini-TARs) [6,7], are widespread and can provide invaluable information on the geological history of the landing site, a possibility that has not been explored so far. In this study, we investigate the relationship between TARs and an enigmatic EW-oriented ridge pattern that is pervasive across the ExoMars landing area [8] (Fig. 1) by using HiRISE images and DTMs [9]. We test the hypothesis of an aeolian origin for these ridges and discuss the related climatic implications.

TARs: TARs/mini-TARs are inactive bedforms as suggested by the presence of superimposed craters. The general trend of these bedforms in Oxia Planum, derived by mapping of 1370 TARs crestlines in sampling areas, is NE-SW (53.9 ± 13.2°) (Fig. 1b). A set of dark and bright alternating bands following the TAR topography are locally visible over the southeastern TAR slopes. We interpret these layers as exposed cross beds over the erosional stoss side [10-12] indicating formative wind direction from the SE. TARs and mini-TARs overlie a set of cratered ridges that cover 44% of the presumed landing area (~633 km^2).

Ridges: Ridges display Y-junctions, are on average 38-meters spaced, trend ~EW (95.4 ± 10°) and are 0.5-1.5-meter-tall (Fig.1a, b). Ridges are bright-toned, show cross-cutting fractures and share the same blocky texture of the bedrock they are associated with (Fig. 1a, c). Ridge crestlines are locally found in continuity outside and inside heavily eroded impact craters around the dark upstanding material exposed in the center of many craters (Fig. 2a). The dark material is the volcanic dark resistant unit (Adru) emplaced at the crater floor and outcropping as the inverted, flat-topped morphology visible nowadays [4].

Ridges are even visible in association with impact crater ejecta and are superimposed by 10-25 m craters and boulders, so they pre-date these impact events (Fig. 1c). When associated with crater ejecta, ridges locally show two different crests (Fig. 2b). Both crests are truncated by craters, which suggest that the double crest arrangement was emplaced before the impacts (Fig. 2c). To better understand the relative age of the ridges, we mapped their occurrence on 316 craters in the study area that we qualitatively classified as relatively degraded/old and pristine/young on the basis of their state of degradation. Results show that ridges are only found in degraded/old craters but are never found inside pristine/young craters. Thus, the ridge forming process was only active in-between the formation of degraded/old and pristine/young craters.

An aeolian (PBR) origin for the ridges: Here we interpret the ridge unit as periodic bedrock ridges (PBRs), which are bedform-like erosional features [13] seeded by megaripples [14]. The stratigraphic relationships between PBRs and craters suggest that these PBRs postdate the emplacement of the Adru in the Early Amazonian and even the subsequent erosion of the old crater rims in the study site. Ejecta material from following impacts favored the preservation of the PBR-seeding megaripples which are locally visible on the southern edges of the PBRs (Fig. 2b, c). Thus, the wind that formed the megaripple-PBR system should have blown from N-NNE because the megaripples are located at the downwind side of PBRs [14] (Fig. 2c). The ejecta deposited over the megaripple-PBRs favored the preservation of the megaripple crests from a subsequent episode/s of erosion that lead to the complete exposure of the PBRs on the plain.

A major change in the wind regime occurred during or after the event that exposed the PBRs: N-NNE winds that shaped the PBRs changed into dominant SE winds that led to the deposition of the TARs/mini-TARs population above the PBR/megaripples, forming the complex pattern [15] still visible today (Fig. 2a).

Conclusions: This work unveils a complex history of aeolian erosion and deposition in Oxia Planum during the Amazonian. The PBR orientation differs from younger TARs/mini-TARs suggesting that the wind regime changed from mostly dominant N winds to

dominant SE winds. Stratigraphic relationships indicate that the erosion of PBRs occurred after the emplacement of a dark volcanic unit in the Early Amazonian and halted before the formation of pristine-looking impacts. By visiting PBRs for the first time, the ExoMars 2022 mission will provide further constraints on PBR formation and paleo-winds, shedding light on a past Amazonian environment.

This work is a summary of a manuscript that is currently in press on Geophysical Research Letters: Silvestro et al. 2021, Periodic Bedrock Ridges at the ExoMars 2022 Landing Site: Evidence for a Changing Wind Regime. DOI: 10.1029/2020GL091651.

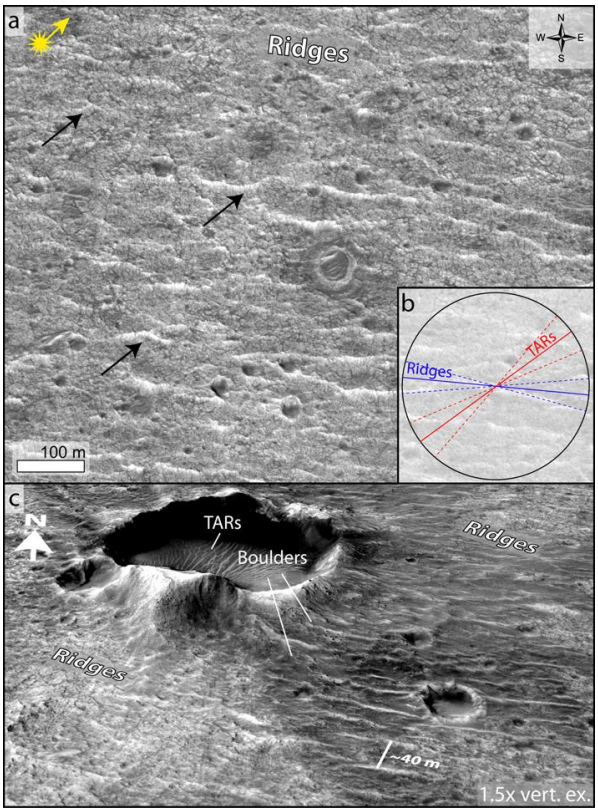

Fig. 1: a) HiRISE image (ESP_039299_1985) showing the ridge unit. Y junctions are clearly visible (black arrows). **b)** Circular plot showing the average trend and circular standard deviation intervals of the mapped ridges and TARs. **c)** HiRISE perspective views of the ridge unit (ESP_036925_1985). Note the superposition of small craters and boulders from the nearby impacts.

References: [1] Vago J. et al. (2015). *SSR, 49(7),* 518–528. [2] Vago J. et al. (2017). *Astrobiology, 17(6–7),* 471–510. [3] Rodionov D. et al. (2017). *Sixth Int. Work. on the Mars Atm.*, 3–5. [4] Quantin-Nataf C. et al. (2021). *Astrobiology, 21*, N.3. [5]. Carter J. et al. (2016). *47th LPSC*, (2016), 2064. [6] Balme M. et al. (2017). *PSS, 153*, 39–53. [7] Bhardwaj A. et. al. (2019). *Remote Sens., 11(8),* 1–17. [8] Silvestro S. et al. (2020). *6th Int. Planet. Dunes Work.* 12-15 May, 2020. LPI No. 2188, id.3009. [9] McEwen A. et al. (2007). *JGR, 112(E5),* E05S02. [10] Golombek M. et al. (2010). *JGR, 115*, 1–34. [11] Arvidson R. E. et al. (2011). *JGR, 116*, 1–33. [12] Geissler P. E. (2014). *JGR, 119(12).* [13] Montgomery D. R. et al. (2012). *JGR, 117*(E3), E03005. [14] Hugenholtz C. H. et al. (2015). *Aeolian Res. 18*, 135–144. [15] Kocurek G. A. & Ewing R. C. (2005). *Geomorph. 72*(1–4), 94–105.

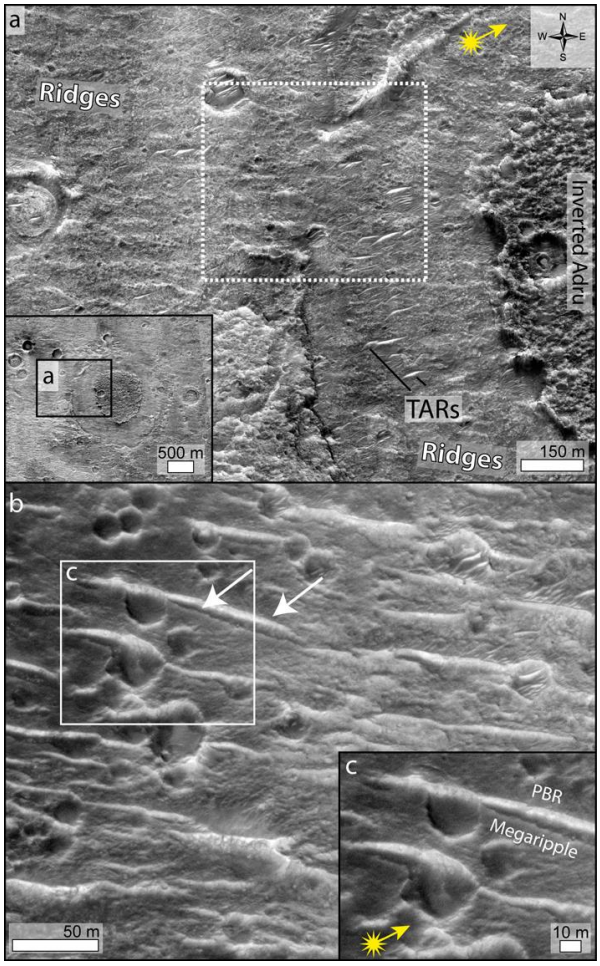

Fig. 2: a) HiRISE image (ESP_050560_1980) showing the mutual stratigraphic relationship between large eroded impacts, ridges, dark resistant unit (Adru) and TARs. Note the continuity of the ridge crestlines inside and outside the crater rim (white dashed box) and the younger TARs overlying the ridges (location in inset on the bottom left). **b)** HiRISE image of the double crest structure (white arrows) interpreted as megaripples detaching from PBRs and suggesting formative winds from the NNE (ESP_050560_1980). **c)** Detail of the double crest structures, note the craters cutting both the PBR and megaripple crests.